J Mater Sci: Mater Med (2010) 21:1703–1712
DOI 10.1007/s10856-010-4030-8

Lens epithelial cell response to atmospheric pressure plasma modified poly(methylmethacrylate) surfaces

Raechelle A. D'Sa · George A. Burke · Brian J. Meenan

Received: 16 November 2009 / Accepted: 8 February 2010 / Published online: 27 February 2010

Abstract Selective control of cellular response to polymeric biomaterials is an important consideration for many ocular implant applications. In particular, there is often a need to have one surface of an ophthalmic implant capable of promoting cell attachment while the other needs to be resistant to this effect. In this study, an atmospheric pressure dielectric barrier discharge (DBD) has been used to modify the surface region of poly(methyl methacrylate) (PMMA), a well established ocular biomaterial, with the aim of promoting a controlled response to human lens epithelial cells (LEC) cultured thereon. The DBD plasma discharge environment has also been employed to chemically graft a layer of poly(ethylene glycol) methyl ether methacrylate (PEGMA) onto the PMMA and the response to LEC likewise determined. Two different molecular weights of PEGMA, namely 1000 and 2000 MW were used in these experiments. The LEC response to DBD treated polystyrene (PS) samples has also been examined as a positive control and to help to further elucidate the nature of the modified surfaces. The LEC adhered and proliferated readily on the DBD treated PMMA and PS surfaces when compared to the pristine polymer samples which showed little or no cell response. The PMMA and PS surfaces that had been DBD grafted with the PEGMA$_{1000}$ layer were found to have some adhered cells. However, on closer inspection, these cells were clearly on the verge of detaching. In the case of the PEGMA$_{2000}$ grafted surfaces no cells were observed indicating that the higher molecular weight PEGMA has been able to attain a surface conformation that is capable of resisting cell attachment in vitro.

R. A. D'Sa · G. A. Burke · B. J. Meenan (✉)
Nanotechnology and Integrated Bio-Engineering Centre (NIBEC), School of Engineering, University of Ulster, Shore Road, Co Antrim, BT37 0QB Newtownabbey, Northern Ireland
e-mail: bj.meenan@ulster.ac.uk

1 Introduction

In normal vision, light passes through the transparent cornea and lens before arriving at the retina. Opacification of either the cornea or lens can result in monocular blindness with the naturally occurring corneas or lenses needing to be surgically replaced by a keratoprostheses or intraocular lenses, respectively [1]. Failure of an implanted keratoprosthesis can occur due to weakening at host–implant interface often caused by poor cell adhesion, or due to fibrous membrane development on the interior of the implant [2]. Requirements, for the fabrication of a functional keratoprosthesis necessitates that the biomaterial to be able to spatially control cell adhesion. The ideal biomaterial surface in this context must provide enhanced cell attachment at the host–implant interface while promoting reduced protein and cell adhesion on the interior of the implant to ensure longevity in vivo [2–5]. In the case of intraocular lenses, failure of the implant generally results from residual lens epithelial cells (LECs) migrating along the capsule and inducing posterior capsular opacification (PCO), a process that can occur long after successful surgery [6]. Various research approaches have been used in an attempt to eliminate PCO [6, 7]. One strategy is to use a biomaterial which gives the implant the ability to resist protein and cellular adhesion [8–12].

This study reports on the use of an atmospheric pressure surface modification procedure that employs a dielectric barrier discharge (DBD) to modify the surface properties of polymeric biomaterials in a manner that allows for control of cellular response thereon. Poly(methyl methacrylate)

(PMMA) is used widely for the fabrication of ocular devices and was chosen here as a model substrate for the surface modification processes of interest. Polystyrene (PS) is a well established substrate for cell culture and was used in these studies as a positive control to further elucidate the effects of the DBD grafting on cell response. The hydrophilic surfaces obtained by plasma modification have been proven to produce conditions that are conducive to increased cellular response [13–16].

It is well accepted that grafting of poly(ethylene glycol) (PEG) onto a substrate generally results in a reduction in the adherence of proteins and cells onto its surface [17–22]. Previous work has illustrated a novel way of chemically grafting non-fouling methacrylate terminated PEG (PEGMA) layers onto polymer surfaces via DBD plasma induced grafting [23]. Whereas, plasma processing has been used to graft molecules onto substrates, it is not widely applied due to the high engineering costs associated with vacuum-based plasmas that are normally required to carry out these reactions [24–27]. In this regard, DBD processing offers an attractive alternative since it allows for rapid, continuous in-line processing and lower operational costs as it functions under atmospheric pressure conditions. The PEGMA grafted surfaces that can be produced by this type of cold plasma processing method have already been shown to resist protein adhesion. The effects that the PEGMA-grafted PMMA and PS surfaces have on lens epithelial cell response in vitro are presented here.

2 Materials and methods

2.1 Atmospheric pressure DBD treatment

Surface treatment was carried out at atmospheric pressure using a laboratory scale DBD system (Arcojet Gmbh, Germany). Commercial grade PMMA (1 mm thick) and PS (1.2 mm thick) sheets (Goodfellow, Cambridge, UK) were used as the polymer substrates for these studies. Discs of 34 mm diameter were punched from the polymer for use in all the cell culture studies and associated assays with the exception of the immunofluorescence staining studies which used 22 mm diameter discs. Samples were cleaned by sonication in ethanol for 15 min and dried in air overnight prior to use.

The DBD system is shown schematically in Fig. 1 and has been described in detail elsewhere [28–34]. In brief, polymer samples were placed on a 2 mm thick rubber covered aluminium platen which constitutes the ground electrode. The plasma discharge was then generated by moving the platen/substrate assembly under three stationary tubular metal electrodes of diameter of 11.8 mm each arranged in parallel to create a 2 mm wide gap between the two components. The three working electrodes are driven by a sinusoidal high voltage AC power supply at a frequency in the range 40–80 kHz. The action of sliding the ground electrode under the working electrodes automatically creates the active discharge zone. Exposure of the polymer samples to the atmospheric pressure plasma discharge can be described quantitatively by two parameters namely: the power density (P_d), and the residence time of the substrate in the plasma (R). The total energy delivered by the plasma to the substrate surface per unit area can therefore be give as the dose ($D = 2NP_d/vl$) in J/cm^2 where l, is the length of the discharge region and N is the number times the platen slides back and forth (referred to as a cycle) through the discharge zone with a transit speed denoted v. Each cycle is equivalent to two periods of exposure (i.e. forward and backward). For the purposes of this study, the power was fixed at 500 W and the values of D are reported with the relevant values of P_d and R provided for completeness.

2.2 Preparation of PEGylated surfaces

PEGylated PMMA and PS surfaces were prepared at atmospheric pressure via processing of substrates exposed to solutions of PEGMA in the DBD reactor as previously

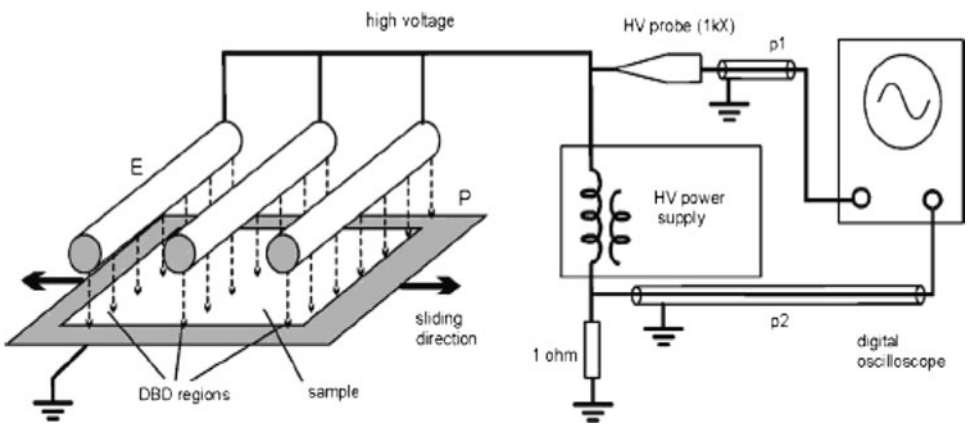

Fig. 1 Schematic of in house dielectric barrier discharge setup

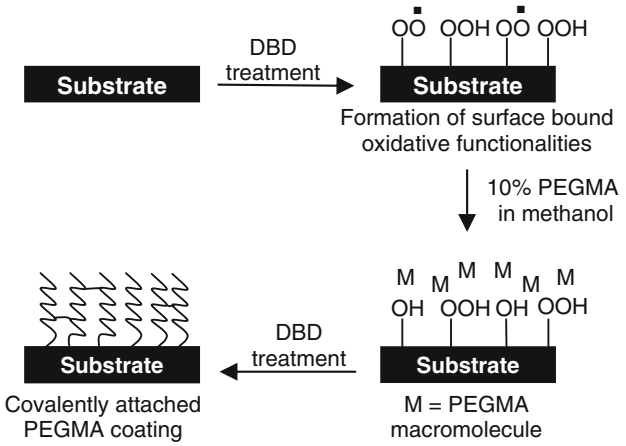

Fig. 2 Schematic illustration of plasma graft induced polymerisation onto PMMA and PS

described [23] and shown schematically in Fig. 2. In brief, the MW: 1000 and 2000 Da PEGMA materials were dissolved in methanol (Sigma-Aldrich, UK) at a concentration of 10% w/v. The polymer surfaces of interest were DBD treated followed by immediately dip coating the samples in the PEGMA–methanol solution for 10 s. The coated polymers were allowed to dry in an oven at 50°C for 2 h and subsequently DBD treated. The samples were then washed repeatedly with methanol and submersed in Milli-Q ultrapure water for 16 h on a rocker table to remove any non-covalently bound PEGMA. Samples were dried under a stream of nitrogen and stored in sterile Petri dishes prior to analysis. The sample nomenclature adopted is: untreated (control), DBD treatment prior to $PEGMA_{1000}$ grafting ($PMMA_{OX}'$, PS_{OX}'), DBD treatment prior to $PEGMA_{2000}$ grafting ($PMMA_{OX}''$, PS_{OX}''), $PEGMA_{1000}$ grafting (PMMA-*g*-$PEGMA_{1000}$, PS-*g*-$PEGMA_{1000}$) and $PEGMA_{2000}$ grafting (PMMA-*g*-$PEGMA_{1000}$, PS-*g*-$PEGMA_{2000}$). The treatment parameters are given in Table 1.

2.3 Biological analysis

2.3.1 Cell culture

Samples that were variously DBD processed were placed in a laminar flow hood and left to relax for 48 h. A stock solution of 0.6% Agar (Sigma-Aldrich, UK) in Milli-Q water was freshly prepared and autoclaved at 160°C for 2 h. Hot Agar (2 cm^3) was pipetted into sterile six well plates followed by careful placement of the polymer samples. Agar was used as a gelling agent to stick the polymeric substrates to the six well plates in order to avoid cells adhering to the under side of the substrates and the tissue culture polystyrene (TCPS).

Immortalised human LECs (CRL-11421) were used to assess the response of air DBD processed surfaces in cell culture. Cells were grown in a humidified atmosphere of 5% CO_2 in Eagle's minimum essential medium (MEM, Gibco, UK) that was supplemented with 10% foetal bovine serum (FBS), 100 IU/ml penicillin G, 100 μg/ml streptomycin sulphate, and 20 μg/ml gentamycin (all obtained from Invitrogen, UK). The cells were maintained at below 70% confluency and were passaged every 3–4 days using 0.25% trypsin–EDTA (Sigma, UK) into 75 cm^3 (T-75) tissue culture flasks. The cells were seeded on PMMA and PS polymer discs at a concentration of 2×10^6 cells and the samples then cultured under normal humidified conditions at 37°C, 5% CO_2 for 4, 24 and 48 h, respectively. Cell media was changed every 2 days. All assays were carried out in triplicate and repeated three times to confirm results.

2.3.2 Crystal violet adhesion assay

LECs were seeded onto the polymer samples in the agar loaded six well plates and incubated for 4 h at 37°C in a humidified 5% CO_2 atmosphere. The media was aspirated

Table 1 Experimental conditions for DBD treated and PEGMA grafted polymer substrates

Substrate nomenclature	DBD modification/pre-treatment			Grafting molecule MW	DBD grafting treatment		
	D (J/cm^2)	P_d (W/cm^2)	R (s)		D (J/cm^2)	P_d (W/cm^2)	R (s)
PS							
PS_{ox}'	314.9	5.3	56.6				
PS_{ox}''	105.0	5.3	18.8				
PS-*g*-$PEGMA_{1000}$	314.9	5.3	56.6	1000	314.9	5.3	56.6
PS-*g*-$PEGMA_{2000}$	105.0	5.3	18.8	2000	105.0	5.3	18.8
PMMA							
$PMMA_{ox}'$	210.0	5.3	37.5				
$PMMA_{ox}''$	105.0	5.3	18.8				
PMMA-*g*-$PEGMA_{1000}$	210.0	5.3	37.5	1000	210.0	5.3	37.5
PMMA-*g*-$PEGMA_{2000}$	105.0	5.3	18.8	2000	105.0	5.3	18.8

off and the cells were washed twice with PBS and morphologically fixed and permeabilised in a solution of 3.7% paraformaldehyde (PFA)/0.01% Triton-X in PBS, respectively. After 20 min the cells were washed with PBS and incubated with 2 cm^3 of 0.5% crystal violet aqueous solution for 30 min. The samples were washed with copious amount of Milli-Q water and the stained cells were solubilised with 1 cm^3 of 2% sodium dodecyl sulphate (SDS) for 16 h to allow for complete solubilisation of the dye taken up by the cells. Aliquots of 200 µl of this solution pertaining to each sample type were transferred in triplicate to a 96-well plate, giving a total of nine replicates per sample type. The absorbance of the solution (optical density) was read in a Tecan Sunrise™ (TECAN Austria GmbH) microplate reader (equipped with Magellan Software) using a 570 nm filter.

2.3.3 MTT cell viability assay

A stock solution of 5 mg/cm^3 MTT [3-(4,5-dimethylthiazol-2-yl)-2,5-diphenyltetrazolium bromide] (Sigma-Aldrich, UK) was prepared in PBS and was passed through a 0.2 mm filter and stored at 2°C. Cells were grown on substrates following culture passage. After 24 and 48 h of cell seeding on surfaces, the culture media was replaced with phenol red free Earles's MEM (Gibco, UK) media. Aliquots of 20 µl of the MTT stock solution added to each well giving a 10% working volume of MTT. The cells were incubated at 37°C in a humidified 5% CO_2 atmosphere until the formazan product was visible ($\sim$2.5 h). The culture medium was aspirated off and the cells were solubilised with 1 cm^3 of 2% SDS for 16 h. Aliquots of 200 µl pertaining to each sample type were transferred in triplicate to a 96-well plate, giving a total of nine replicates per sample type. Absorbance (optical density) was read in a Tecan Sunrise™ (TECAN GmbH, Austria) microplate reader equipped with Magellan Software using a 570 nm filter.

2.3.4 Immunocytochemistry

Cells were grown on substrates for 24 h following culture passage. Large volumes of ice-cold PBS were used to rinse the cells (3 × 5 min), prior to fixing them 3.7% PFA/PBS and solubilising with 0.1% Triton X-100/PBS at 4°C. After 20 min the cells were washed with PBS (3 × 5 min) to remove any traces of PFA. To visualize actin, samples were then incubated with phalloidin Alexa Fluor 488 (Molecular Probes, UK) at 25 U/cm^3. The samples were rinsed in PBS (3 × 5 min) and mounted with Vectashield Mounting Medium containing 1.5 µg/cm^3 of DAPI counterstain (Vector Laboratories, UK). A clear varnish was used to seal the slides and they were examined using a Carl Zeiss LSM5 Pascal (Carl Zeiss MicroImaging, Germany) Confocal Laser Scanning Microscope.

2.3.5 Image analysis

Images were loaded into NIH ImageJ Software (v 1.38× NIH, USA). Cell counts were performed by quantifying the DAPI stained cell nuclei from six random fields of view taken for each sample type. All samples were run in triplicate.

2.3.6 Statistical analysis

The statistical analysis of all the surface analysis and biological assays was performed with Origin® (v. 7.0383, OriginLab Corporation, USA). One way analysis of variance (ANOVA) was used to compare mean values in order to determine equivalence of variance between pairs of samples. Significance between groups was determined using the Bonferroni multiple comparison test. A value of $P < 0.05$ was taken as statistically significant. Results are reported as means ± standard deviation. All experiments were carried out in triplicate and repeated.

3 Results and discussion

3.1 Cell adhesion

The chemical and microstructural effects of DBD treatment on PMMA and PS, as well as the properties of PEGMA grafted surfaces was confirmed by contact angle measurement, X-ray photoelectron spectroscopy (XPS), time-of-flight secondary ion mass spectrometry (ToF-SIMS) and atomic force microscopy (AFM) as reported in detail elsewhere [23]. The efficiency of PEGMA grafting was mainly determined through XPS analysis. DBD induced grafting of the two different MW PEGMA results in the occurrence of a characteristic ether (C–O–C) carbon component at 286.5 eV in the C1s region of the XPS spectra. An increase in the intensity of this C–O–C component is deemed to be indicative of the presence of more PEGMA having been grafted onto the PS surface. The most optimised PEGMA grafted studies are used here. The PMMA-*g*-$PEGMA_{1000}$ and PMMA-*g*-$PEGMA_{2000}$ had 61.8 and 81.6 at.% C–O–C component in the C1s region of the XPS spectra, respectively [23]. Likewise, the PS-*g*-$PEGMA_{1000}$, PS-*g*-$PEGMA_{2000}$ had 58.7 and 64.4 at.% C–O–C component in the C1s region of the XPS spectra respectively [23]. The ToF-SIMS images showed PMMA-*g*-$PEGMA_{1000}$ and PS-*g*-$PEGMA_{1000}$ to have a non-coherent coverage on the surface, where as the PMMA-*g*-$PEGMA_{2000}$ and PS-*g*-$PEGMA_{2000}$ were homogenously

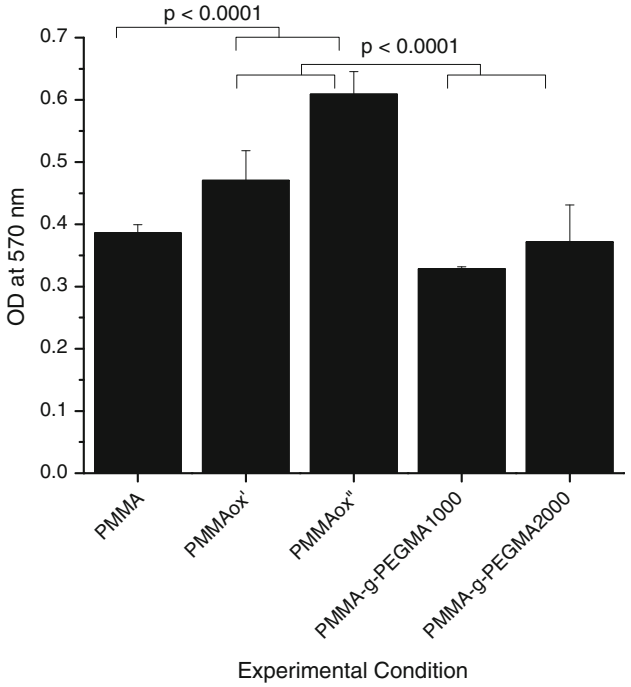

Fig. 3 Crystal violet adhesion assay data for LEC on the various PMMA samples 4 h post-seeding

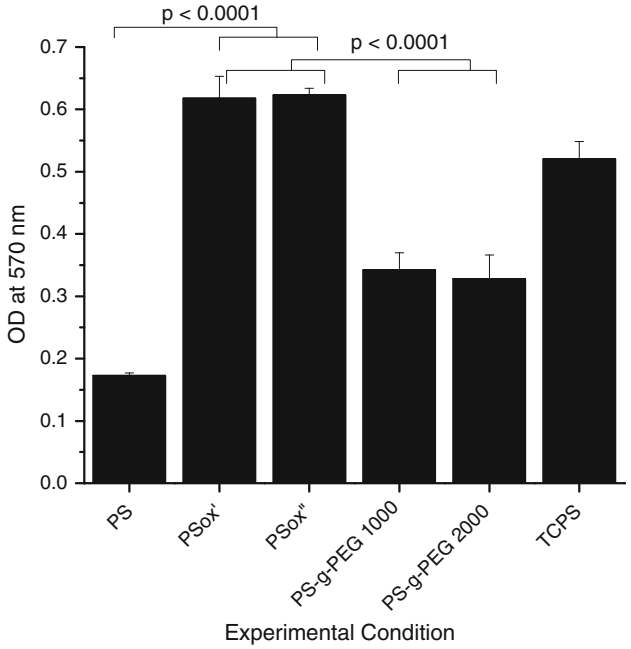

Fig. 4 Crystal violet adhesion assay data for LEC on the various PS samples 4 h post-seeding

grafted on the surface to the detection limit of the technique [23].

The initial attachment of LECs to pristine PMMA, PS; DBD treated surfaces ($PMMA_{ox}'$, $PMMA_{ox}''$, PS_{ox}', PS_{ox}'') and PEGMA grafted surfaces (PMMA-*g*-$PEGMA_{1000}$, PMMA-*g*-$PEGMA_{2000}$, PS-*g*-$PEGMA_{1000}$, PS-*g*-$PEGMA_{2000}$) were quantified 4 h post-seeding. Graphical representations of the results are presented in Figs. 3 and 4. For both polymers, low numbers of LECs were found to attach to the pristine and PEGylated surfaces. Conversely, statistically significant ($P < 0.0001$) greater numbers of cells adhered to the DBD-treated PMMA and PS surfaces ($PMMA_{ox}'$, $PMMA_{ox}''$, PS_{ox}', PS_{ox}''), as in Figs. 3 and 4. Interestingly, both the PS_{ox}' and PS_{ox}'' surfaces had higher cell numbers when compared with TCPS, as shown in Fig. 4.

3.2 Cell viability

The MTT assay was used to determine viability of LECs on the modified surfaces at 24 and 48 h post-seeding with the relevant data presented in Figs. 5 and 6, respectively. Cell viability on the DBD treated polymers ($PMMA_{ox}'$, $PMMA_{ox}''$, PS_{ox}', PS_{ox}'') was statistically higher ($P < 0.0001$) than that on the pristine controls and the PEGylated samples (PMMA-*g*-$PEGMA_{1000}$, PMMA-*g*-$PEGMA_{2000}$, PS-*g*-$PEGMA_{1000}$, PS-*g*-$PEGMA_{2000}$). It is well known that cells need to attach and spread before they can

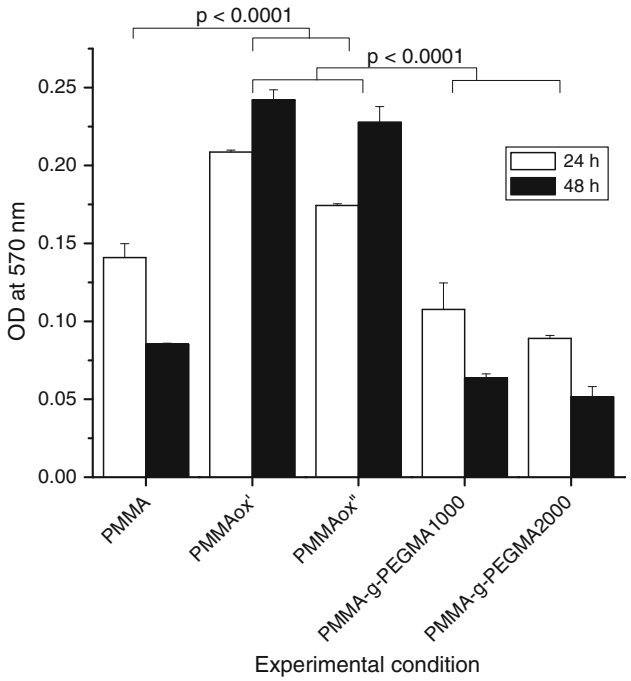

Fig. 5 MTT proliferation assay data for LECs on the various PMMA samples 24 and 48 h post-seeding

undergo proliferation. Hence, these data are consistent with cell adhesion assay results presented above. As such, it is clear that the LECs that have adhered onto the DBD treated surfaces after 4 h in culture are viable and capable of proliferating thereby indicating that this modified surface

condition created allows for an increased cellular response. Alternatively, the results also demonstrate that atmospheric pressure DBD induced grafting of PEGMA onto PMMA and PS creates a surface that is resistant to cell adhesion. Whereas, the $PEGMA_{1000}$ surface does support some cell adhesion, the numbers present are lower than that on the DBD treated samples. For the $PEGMA_{2000}$ surfaces the effect is significantly greater with no detectable cells present. Hence, the $PEGMA_{2000}$ grafted surface condition produced here is promising method for resisting cellular response to polymers.

3.3 Immunocytochemistry

The overall morphology of LEC adhering to the pristine and DBD-treated surfaces was visualised by actin and nuclei staining 24 h post-seeding. Figures 7 and 8 show LECs seeded at the same cell density and culture conditions onto pristine polymer (PMMA, PS), DBD polymer ($PMMA_{ox}'$ and $PMMA_{ox}''$, PS_{ox}', PS_{ox}'') and PEGylated (PMMA-*g*-$PEGMA_{1000}$, PMMA-*g*-$PEGMA_{2000}$, PS-*g*-$PEGMA_{1000}$, PS-*g*-$PEGMA_{2000}$) polymer surfaces. The morphology of the cells varied depending on the substrate type concerned. Cells on the pristine PS and PMMA were partially spread with the direction of the actin stress fibres dominant along the long axis of the cells and reduced numbers of observed fibres in the interior of the cells. These cells displayed a bipolar spindle spaced morphology characterised by a low cell area and high aspect ratio of the type observed previously by Evans et al. for LECs [35]. By contrast, the cells on the DBD treated surfaces had a well spread morphology with a higher contact area. As indicated earlier, there were much greater numbers of cells on these surfaces, particularly on the PS_{ox}' and PS_{ox}'' samples, with a clearly defined hexagonal packing morphology, as reported by Weber and Menko [36]. Consequently, the actin stress fibres from the cells on the DBD treated surfaces formed a dense and complex network. The LECs present on the PMMA-*g*-$PEGMA_{1000}$ and PS-*g*-$PEGMA_{1000}$ surfaces have an obvious rounded morphology many of which are detaching from the substrate leading to collections of cells folding over one another. These cells displayed little or no stress fibre formation, but rather exhibited evidence of pronounced shrinkage and loss of cell–cell contact in a manner similar to results reported by Yan et al. for LEC grown on PMMA and silicone discs [37]. As indicated in the previous section, no cells were detected on the PMMA-*g*-$PEGMA_{2000}$ or PS-*g*-$PEGMA_{2000}$ samples under the experimental conditions used here.

Cells that display a rounded morphology are normally indicative of poor adherence to the substrate. This behaviour can lead to apoptotic cell death and commonly

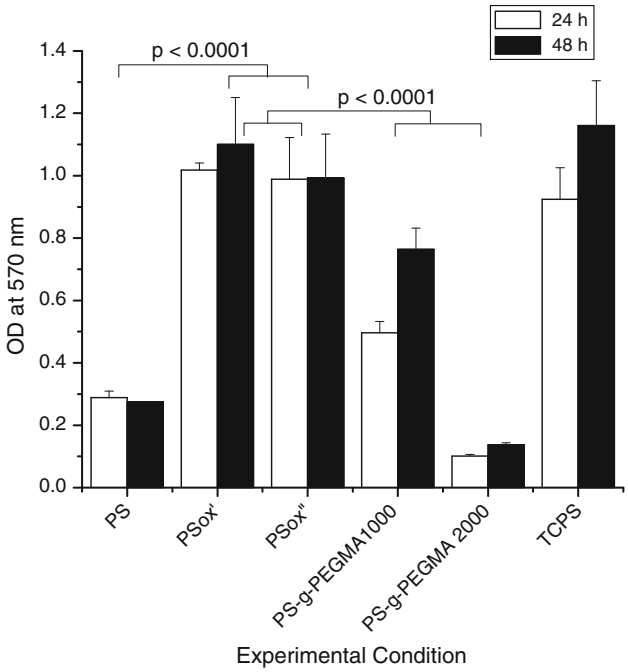

Fig. 6 MTT proliferation assay data for LECs on the various PS samples 24 and 48 h post-seeding

accounts for failure in polymeric implants. Conversely, well spread morphologies are indicative of cells that are adhering and proliferating. Cell spreading involves a rearrangement of the cytoskeletal and membrane components and thereby results in a flattened morphology characterised by actin stress fibres terminating in the focal adhesion points. A stable actin cytoskeletal structure for adherent cells is generally related to well formed attachments to the extracellular matrix (ECM) [38] and interactions with neighbouring cells [39]. Stress fibres that are organised from actin filaments are associated with integrin receptors at the focal adhesion points where they control integrin signalling and integrin/matrix adhesion [40–42]. Weber et al. have observed that the disassembly of actin stress fibres in LEC is concomitant with initiation of lens epithelial cell differentiation, just as is the case for many other cell types [36, 43, 44]. In fact these actin stress fibres in LECs provide a survival signal that inhibits the cells from initiating apoptotic pathways [36]. Since actin stress fibres are responsible for anchorage at the cell adhesion sites, it can be stated that adherence is substantially stronger on the DBD-treated surfaces (with a well spread network of actin fibres) compared to pristine or PEGylated surfaces (displaying few actin fibres), as shown in Figs. 7 and 8.

3.4 Cell counts

Cell counts determined by ImageJ analysis were used to corroborate the colourimetric assays. The DAPI stained

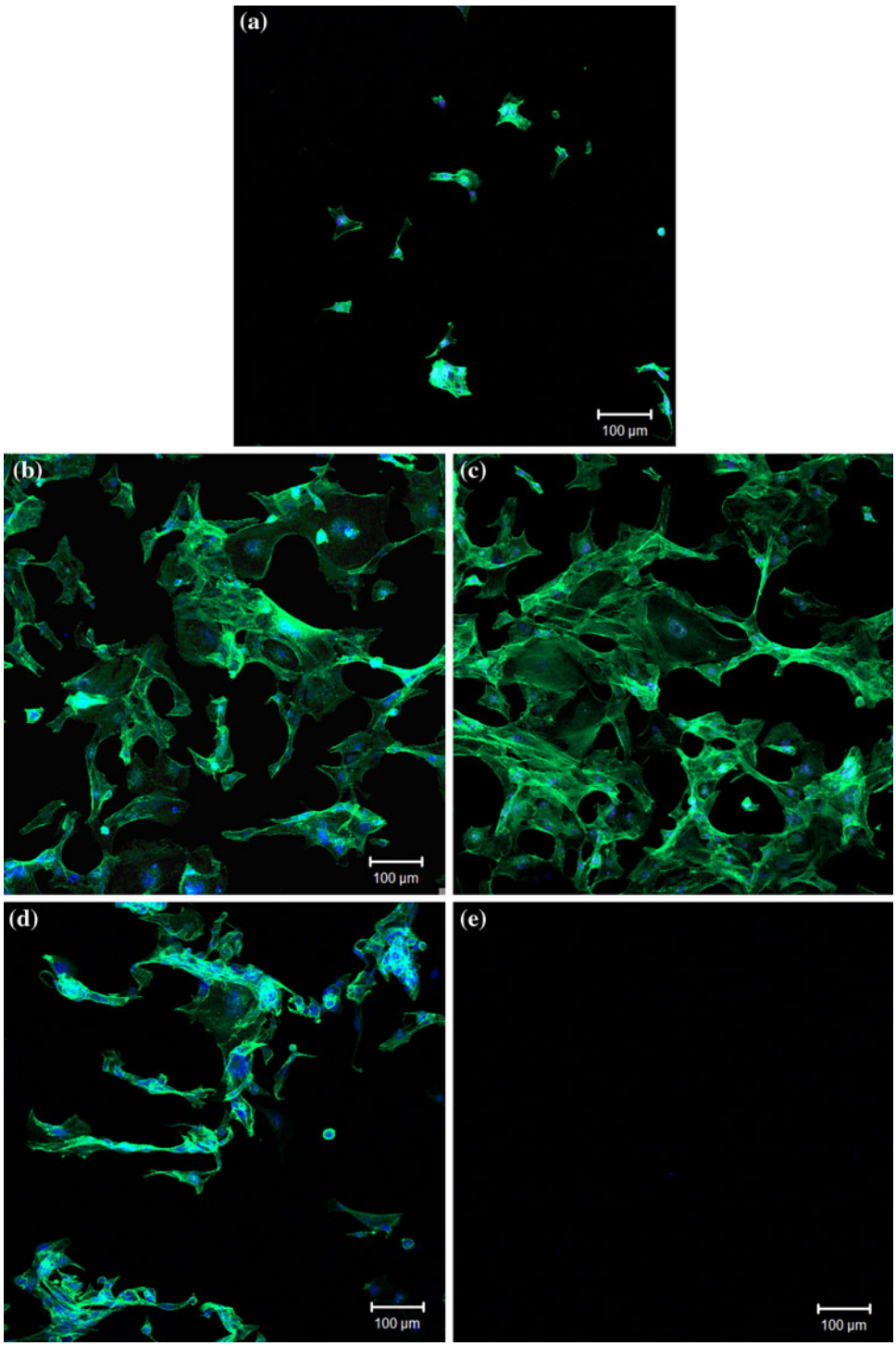

Fig. 7 Confocal micrographs of LECs dual stained with actin (*green*) and nuclei (*blue*) showing the cytoskeleton in cells 24 h post-seeding on after 24 h incubation on **a** PMMA, **b** $PMMA_{ox}'$, **c** $PMMA_{ox}''$, **d** PMMA-*g*-$PEGMA_{1000}$, **e** PMMA-*g*-$PEGMA_{2000}$. (Color figure online)

nuclei from six random fields of view of each surface condition PMMA and PS samples were counted with the results presented in Figs. 9 and 10. These results confirm those obtained from the colourimetric assays, i.e. cell growth on the DBD pre-treated surfaces is significantly larger ($P < 0.0001$) than that of the PMMA and PS control surfaces. Although there is some cell growth on the PMMA-*g*-$PEGMA_{1000}$ and PS-*g*-$PEGMA_{1000}$ substrates, they are significantly reduced in comparison to their DBD-pre-treated substrates. The cell counting method confirms that there is no cell attachment on the PMMA and PS grafted with $PEGMA_{2000}$. The salient point here is that the PEGylated surfaces were created by a simple DBD induced grafting procedure onto the DBD treated surfaces which themselves show a substantially increased rate of LECs adhesion and viability.

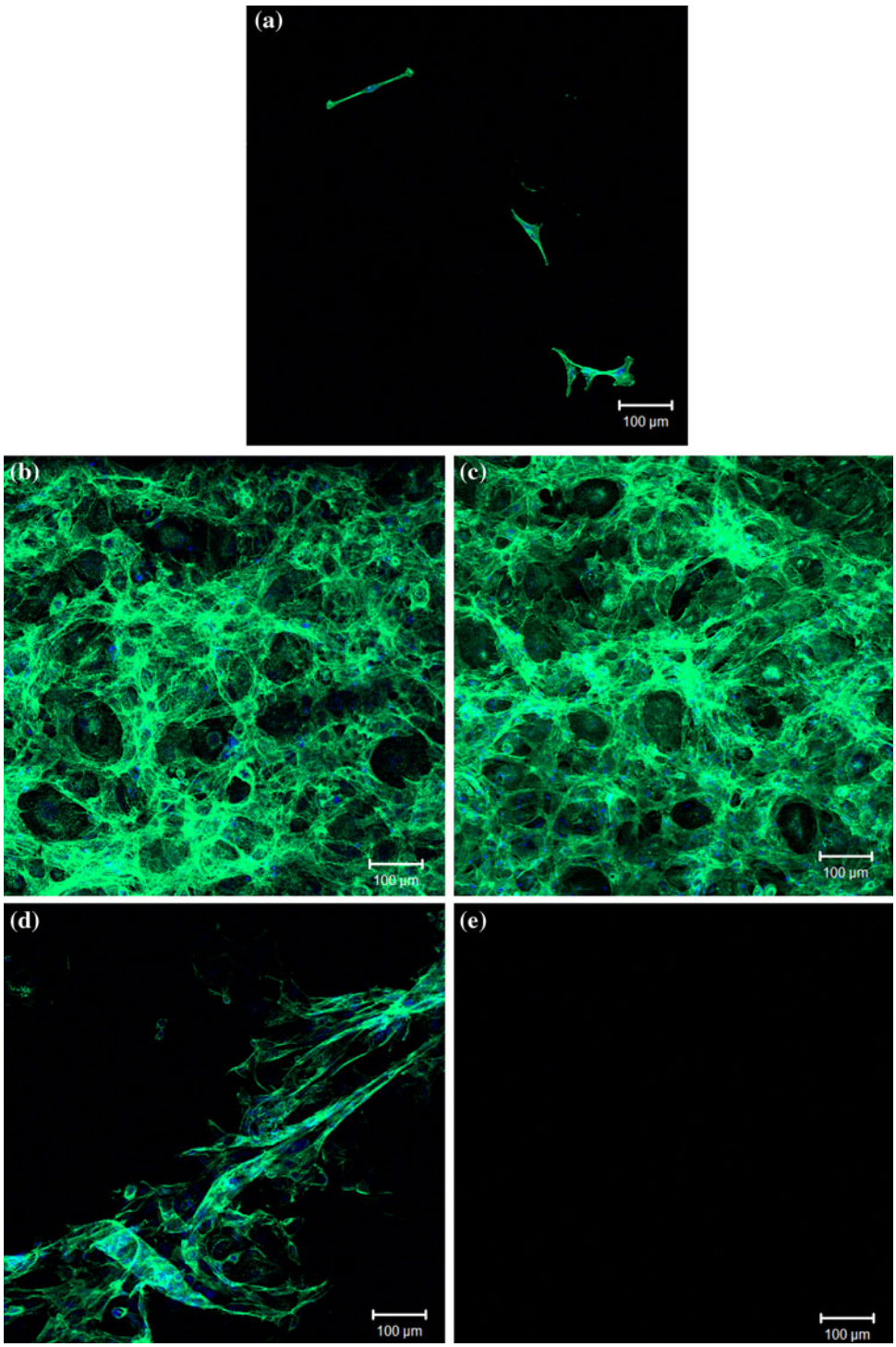

Fig. 8 Confocal micrographs of LECs dual stained with actin (*green*) and nuclei (*blue*) showing the cytoskeleton in cells 24 h post-seeding on **a** PS, **b** PS_{ox}', **c** PS_{ox}'', **d** PS-*g*-$PEGMA_{1000}$, **e** PS-*g*-$PEGMA_{2000}$. (Color figure online)

Control of cellular response can increase the longevity of the implanted medical devices such as keratoprostheses and intraocular lenses. An increase in cellular response is a key requirement for the effective integration of an implanted keratoprosthesis into the corneal stroma, therefore increasing the speed of stabilization and enhancing the long term survival of the implant. Conversely, failure intraocular lenses generally results from residual LECs migrating along the capsule and inducing PCO. In this regard, a surface that resists cell adhesion and proliferation is preferred. The $PEGMA_{2000}$ surfaces produced here by DBD induced chemical grafting suggest themselves as a means to create these conditions using the same atmospheric pressure plasma processing technology. Furthermore, previous work has shown that the $PEGMA_{2000}$ layers are tethered spatially close together on the surface to

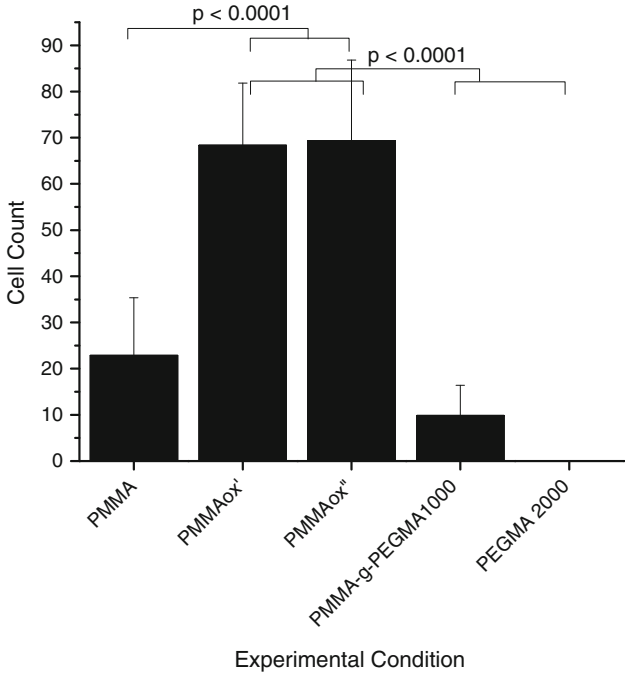

Fig. 9 Cell counts from ImageJ analysis for LEC on the various PMMA samples 24 h post-seeding

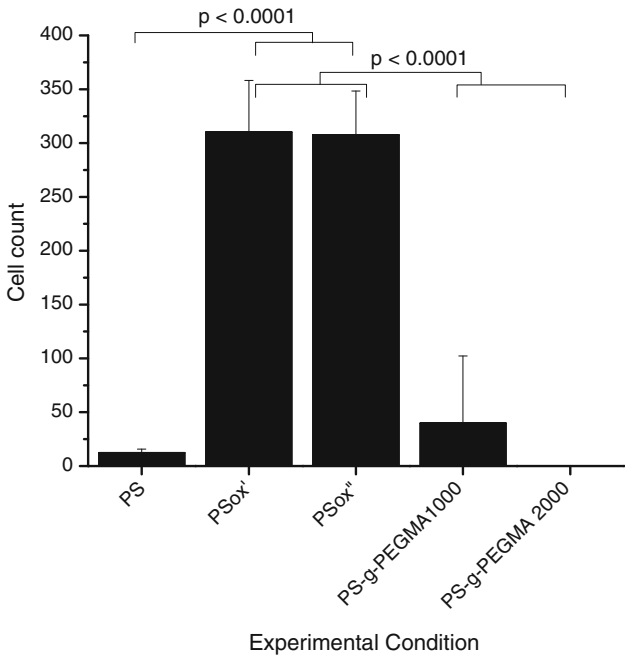

Fig. 10 Cell counts from ImageJ analysis for LEC on the various PS samples 24 h post-seeding

provide for the excluded volume effect [23]. Protein adsorption studies of these $PEGMA_{2000}$ layers has shown this coating to be protein resistant to the detection limit of the technique. As no protein adsorption is observed, the $PEGMA_{2000}$ surfaces do not allow for the Vroman effect [45] which involves a series of competitive protein adsorption events that is followed by attachment proteins adsorbing onto the surface and promoting effective cell adhesion. As blood–material interactions and inflammatory response are also dependant on this well-known Vroman effect of protein adsorption, it is expected that these effects will be minimal on the $PEGMA_{2000}$ grafted surfaces.

4 Conclusions

All biomaterials and by association the implant devices that are made from them, develop a protein coating as soon as they are introduced into a biological environment. As such, cells that subsequently come into contact with such a surface do not "see" a naked surface, but rather are influenced by the nature of this protein adlayer which in turn can be affected by the nature of the substrate surface chemistry. Hydrophilic surfaces allow for a series of protein adsorption events to occur, which eventually allows for effective cell adhesion or otherwise. The nature of actin stress fibres that normally anchor cells to the ECM can be used as an indicator of their response in a given environment. In these studies, actin stress fibres are found to form complex and well defined networks on the DBD treated PMMA and PS surfaces. By comparison, the actin stress fibres for LECs that adhere to the pristine polymer surfaces or the $PEGMA_{1000}$ PEGylated surfaces are not fully formed. This indicates that the DBD treatment method can be used to provide for enhanced cell adhesion and viability. Alternatively, the polymeric samples produced by DBD induced grafting from solutions of $PEGMA_{2000}$ showed no detectable cell adhesion and therefore meets the requirements for non-fouling surfaces. The ability of the DBD technology to modulate increased or decreased cellular response has very exciting implications for the design and surface engineering of implanted ocular biomaterials.

Acknowledgements The authors wish to thank Dr. G. Mahon, Department of Ophthalmology, Queen's University Belfast, UK for provision of the lens epithelial cell line. R. A. D. acknowledges the University of Ulster for the award of a Vice-chancellors postgraduate studentship.

References

1. Lloyd AW, Faragher RG, Denyer SP. Ocular biomaterials and implants. Biomaterials. 2001;22(8):769–85.
2. Ilhan-Sarac O, Akpek EK. Current concepts and techniques in keratoprosthesis. Curr Opin Ophthalmol. 2005;16(4):246–50.
3. Hicks CR, Fitton JH, Chirila TV, Crawford GJ, Constable IJ. Keratoprostheses: advancing toward a true artificial cornea. Surv Ophthalmol. 1997;42(2):175–89.
4. Patel S, Thakar RG, Wong J, McLeod SD, Li S. Control of cell adhesion on poly(methyl methacrylate). Biomaterials. 2006; 27(14):2890–7.

5. Kim MK, Park IS, Park HD, Wee WR, Lee JH, Park KD, et al. Effect of poly(ethylene glycol) graft polymerization of poly (methyl methacrylate) on cell adhesion. In vitro and in vivo study. J Cataract Refract Surg. 2001;27(5):766–74.
6. Spalton DJ. Posterior capsular opacification after cataract surgery. Eye. 1999;13(Pt 3b):489–92.
7. Nishi O. Posterior capsule opacification. Part 1. Experimental investigations. J Cataract Refract Surg. 1999;25(1):106–17.
8. Schauersberger J, Amon A, Kruger A, Abela C, Schild G, Kolodjaschna J. Lens epithelial cell outgrowth on 3 types of intraocular lenses. J Cataract Refract Surg. 2001;27(6):850–4.
9. Yuen C, Williams R, Batterbury M, Grierson I. Modification of the surface properties of a lens material to influence posterior capsular opacification. Graefes Arch Clin Exp Ophthalmol. 2006; 34(6):568–74.
10. Tognetto D, Toto L, Sanguinetti G, Cecchini P, Vattovani O, Filacorda S, et al. Lens epithelial cell reaction after implantation of different intraocular lens materials: two-year results of a randomized prospective trial. Ophthalmology. 2003;110(10): 1935–41.
11. Doan KT, Olson RJ, Mamalis N. Survey of intraocular lens material and design. Curr Opin Ophthalmol. 2002;13(1):24–9.
12. Matsushima H, Iwamoto H, Mukai K, Katsuki Y, Nagata M, Senoo T. Preventing secondary cataract and anterior capsule contraction by modification of intraocular lenses. Expert Rev Med Devices. 2008;5(2):197–207.
13. Lampin M, Warocquier C, Legris C, Degrange M, Sigot-Luizard MF. Correlation between substratum roughness and wettability, cell adhesion, and cell migration. J Biomed Mater Res. 1997;36(1):99–108.
14. Mitchell SA, Davidson MR, Bradley RH. Improved cellular adhesion to acetone plasma modified polystyrene surfaces. J Colloid Interface Sci. 2005;281(1):122–9.
15. Chu PK, Chen JY, Wang LP, Huang N. Plasma-surface modification of biomaterials. Mater Sci Eng R. 2002;36(5-6):143–206.
16. Hubbell JA. Surface treatment of polymers for biocompatibility. Annu Rev Mater Sci. 1996;26:365–94.
17. Kingshott P, Thissen H, Griesser HJ. Effects of cloud-point grafting, chain length, and density of PEG layers on competitive adsorption of ocular proteins. Biomaterials. 2002;23(9):2043–56.
18. Lee JH, Lee HB, Andrade JD. Blood compatibility of polyethylene oxide surfaces. Prog Polym Sci. 1995;20(6):1043–79.
19. Harris JM. Poly(ethylene glycol) chemistry. New York: Plenum; 1992.
20. Kingshott P, Griesser HJ. Surfaces that resist bioadhesion. Curr Opin Solid State Mater Sci. 1999;4(4):403–12.
21. Michel R, Pasche S, Textor M, Castner DG. Influence of PEG architecture on protein adsorption and conformation. Langmuir. 2005;21(26):12327–32.
22. Chen H, Zhang Z, Chen Y, Brook MA, Sheardown H. Protein repellant silicone surfaces by covalent immobilization of poly(ethylene oxide). Biomaterials. 2005;26(15):2391–9.
23. D'Sa RA, Meenan BJ. Chemical grafting of poly(ethylene glycol) methyl ether methacrylate onto polymer surfaces by atmospheric pressure plasma processing. Langmuir. 2010;24(3):1894–903.
24. Uyama Y, Kato K, Ikada Y. Surface modification of polymers by grafting. Adv Polym Sci. 1998;137:1–39.
25. Kato K, Uchida E, Kang ET, Uyama Y, Ikada Y. Polymer surface with graft chains. Prog Polym Sci. 2003;28(2):209–59.
26. Zhao B, Brittain WJ. Polymer brushes: surface-immobilized macromolecules. Prog Polym Sci. 2000;25(5):677–710.
27. Wang P, Tan KL, Kang ET, Neoh KG. Plasma-induced immobilization of poly(ethylene glycol) onto poly(vinylidene fluoride) microporous membrane. J Memb Sci. 2002;195(1):103–14.
28. Liu C, Brown NMD, Meenan BJ. Uniformity analysis of dielectric barrier discharge (DBD) processed polyethylene terephthalate (PET) surface. Appl Surf Sci. 2006;252(6):2297–310.
29. Liu C, Brown NMD, Meenan BJ. Statistical analysis of the effect of dielectric barrier discharge (DBD) operating parameters on the surface processing of poly(methylmethacrylate) film. Surf Sci. 2005;575(3):273–86.
30. Liu C, Cui N, Brown NMD, Meenan BJ. Effects of DBD plasma operating parameters on the polymer surface modification. Surf Coat Technol. 2004;185(2–3):311–20.
31. Upadhyay DJ, Cui NY, Meenan BJ, Brown NMD. The effect of dielectric barrier discharge configuration on the surface modification of aromatic polymers. J Phys D Appl Phys. 2005;38(6): 922–9.
32. Borcia G, Anderson CA, Brown NMD. The surface oxidation of selected polymers using an atmospheric pressure air dielectric barrier discharge. Part II. Appl Surf Sci. 2004;225(1–4):186–97.
33. Borcia G, Anderson CA, Brown NMD. The surface oxidation of selected polymers using an atmospheric pressure air dielectric barrier discharge. Part I. Appl Surf Sci. 2004;221(1–4):203–14.
34. Cui NY, Upadhyay DJ, Anderson CA, Meenan BJ, Brown NMD. Surface oxidation of a Melinex 800 PET polymer material modified by an atmospheric dielectric barrier discharge studied using X-ray photoelectron spectroscopy and contact angle measurement. Appl Surf Sci. 2007;253(8):3865–71.
35. Evans MDM, Pavon-Djavid G, Hélary G, Legeais JM, Migonney V. Vitronectin is significant in the adhesion of lens epithelial cells to PMMA polymers. J Biomed Mater Res A. 2004;69A(3): 469–76.
36. Weber GF, Menko AS. Actin filament organization regulates the induction of lens cell differentiation and survival. Dev Biol. 2006;295(2):714–29.
37. Yan Q, Perdue N, Sage EH. Differential responses of human lens epithelial cells to intraocular lenses in vitro: hydrophobic acrylic versus PMMA or silicone discs. Graefes Arch Clin Exp Ophthalmol. 2005;243(12):1253–62.
38. Wiesner S, Legate KR, Fassler R. Integrin–actin interactions. Cell Mol Life Sci. 2005;62(10):1081–99.
39. Angres B, Barth A, Nelson WJ. Mechanism for transition from initial to stable cell–cell adhesion: kinetic analysis of E-cadherin-mediated adhesion using a quantitative adhesion assay. J Cell Biol. 1996;134(2):549–57.
40. Miyamoto S, Teramoto H, Coso OA, Gutkind JS, Burbelo PD, Akiyama SK, et al. Integrin function: molecular hierarchies of cytoskeletal and signaling molecules. J Cell Biol. 1995;131(3): 791–805.
41. Nojima Y, Morino N, Mimura T, Hamasaki K, Furuya H, Sakai R, et al. Integrin-mediated cell adhesion promotes tyrosine phosphorylation of p130Cas, a Src homology 3-containing molecule having multiple Src homology 2-binding motifs. J Biol Chem. 1995;270(25):15398–402.
42. Shattil SJ, Haimovich B, Cunningham M, Lipfert L, Parsons JT, Ginsberg MH, et al. Tyrosine phosphorylation of pp125FAK in platelets requires coordinated signaling through integrin and agonist receptors. J Biol Chem. 1994;269(20):14738–45.
43. McBeath R, Pirone DM, Nelson CM, Bhadriraju K, Chen CS. Cell shape, cytoskeletal tension, and RhoA regulate stem cell lineage commitment. Dev Cell. 2004;6(4):483–95.
44. Woods A, Wang G, Beier F. RhoA/ROCK signaling regulates Sox9 expression and actin organization during chondrogenesis. J Biol Chem. 2005;280(12):11626–34.
45. Andrade JD, Hlady V. Vroman effects, techniques, and philosophies. J Biomater Sci Polym Ed. 1991;2:161–72.